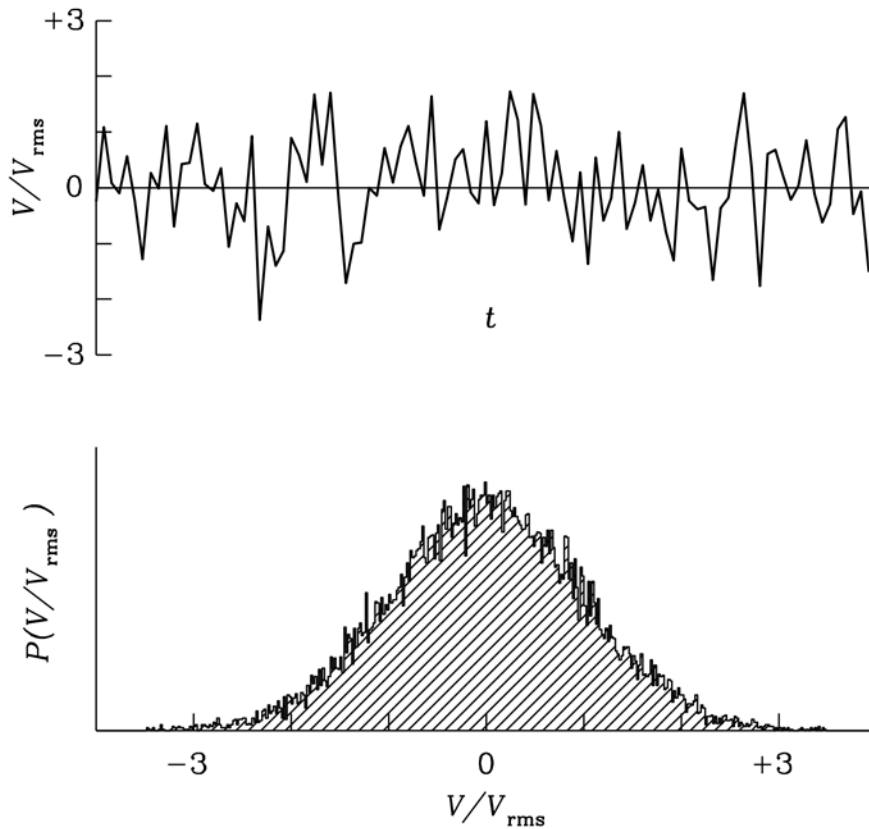


Radiometers

Natural radio emission from the cosmic microwave background, discrete astronomical sources, the Earth's atmosphere, and the ground is random noise that is nearly indistinguishable from the noise generated by a warm resistor or by receiver electronics. A radio receiver used to measure the average power of the noise coming from a radio telescope in a well-defined frequency range is called a **radiometer**. Noise voltage has zero mean and varies randomly on the very short time scales (nanoseconds) comparable with the inverse bandwidth of the radiometer. A square-law detector in the radiometer squares the input noise voltage to produce an output voltage proportional to the input noise power. Noise power is always greater than zero and usually steady when averaged over much longer times (seconds to hours). By averaging a large number N of independent noise samples, an ideal radiometer can determine the average noise power with a fractional uncertainty as small as $(N/2)^{-1/2} \ll 1$ and detect a faint source that increases the antenna temperature by a tiny fraction of the total noise power. The ideal radiometer equation expresses this result in terms of the receiver bandwidth and the averaging time. Gain variations in practical radiometers, fluctuations in atmospheric emission, and confusion by unresolved radio sources may significantly degrade the actual sensitivity compared with the sensitivity predicted by the ideal radiometer equation.

Band-limited noise

The voltage at the output of a radio telescope is the sum of noise voltages from many independent random contributions. The **central limit theorem** states that the amplitude distribution of such noise is nearly Gaussian. The figure below shows the histogram of about 20,000 independent voltage samples randomly drawn from a Gaussian parent distribution having rms V_{rms} and mean $\langle V \rangle = 0$. The sampling theorem (Eq. SF6) states that any signal (even if the "signal" is just noise) of limited bandwidth $\Delta\nu$ and duration τ can be represented by $2N$ independent samples. The figure also shows $N = 100$ successive samples drawn from the Gaussian noise distribution. This sequence of voltages is representative of band-limited noise in the frequency range from 0 to $\Delta\nu$ during a time interval τ such that $\Delta\nu \times \tau = N/2 = 50$, e.g., noise extending to frequency $\Delta\nu = 1$ MHz sampled for $\tau = 50 \mu\text{s}$. This is what the band-limited noise output voltage of a radio telescope looks like.



The output voltage V of a radio telescope varies rapidly on short time scales, as indicated by the upper plot showing 100 independent samples of band-limited noise drawn from a Gaussian probability distribution $P(V/V_{\text{rms}})$ (lower plot) having zero mean and fixed rms V_{rms} .

It is convenient to describe noise power in units of temperature. Since the noise power per unit bandwidth generated by a resistor of temperature T is $P_\nu = kT$ in the low-frequency limit, we can define the **noise temperature** of any noiselike source in terms of its power per unit bandwidth P_ν :

$$T_N \equiv \frac{P_\nu}{k} \quad (3E1)$$

where $k \approx 1.38 \times 10^{-23}$ Joule K⁻¹ is the Boltzmann constant.

The temperature equivalent to the *total* noise power from all sources referenced to the input of an ideal receiver connected to the output of a radio telescope is called the **system noise temperature**. It is the sum of many contributors to the antenna temperature T_A plus the receiver noise temperature T_{rcvr} .

$$T_{\text{sys}} = T_{\text{cmb}} + \triangle T_{\text{source}} + T_{\text{atm}} + T_{\text{spillover}} + T_{\text{rcvr}} + \dots \quad (3\text{E2})$$

The antenna-temperature contributions listed explicitly in Equation 3E2 are $T_{\text{cmb}} \approx 2.73$ K from the cosmic microwave background, $\triangle T_{\text{source}}$ from the astronomical source being observed, T_{atm} from atmospheric emission in the telescope beam, and $T_{\text{spillover}}$ to account for radiation that the feed picks up in directions beyond the edge of the reflector. T_{rcvr} represents the noise power generated by the receiver itself, referenced to the receiver input. All receivers generate noise, and any receiver can be represented by an equivalent circuit consisting of an ideal noiseless receiver whose input is a resistor of temperature T_{rcvr} . Receiver noise is usually minimized by cooling the receiver to cryogenic temperatures.

The astronomical signal $\triangle T_{\text{source}}$ was written with a \triangle to emphasize that it is usually much smaller than the total system noise: $\triangle T_{\text{source}} \ll T_{\text{sys}}$. For example, in the $\nu_{\text{RF}} \approx 4.85$ GHz sky survey made with the 300-foot telescope, the system noise was $T_{\text{sys}} \approx 60$ K, but the faintest sources detected contributed only $\triangle T_{\text{source}} \approx 0.01$ K.

Radiometers

The purpose of the simplest **total-power radiometer** is to measure the timed-averaged power of the input noise in some well-defined radio frequency (RF) range

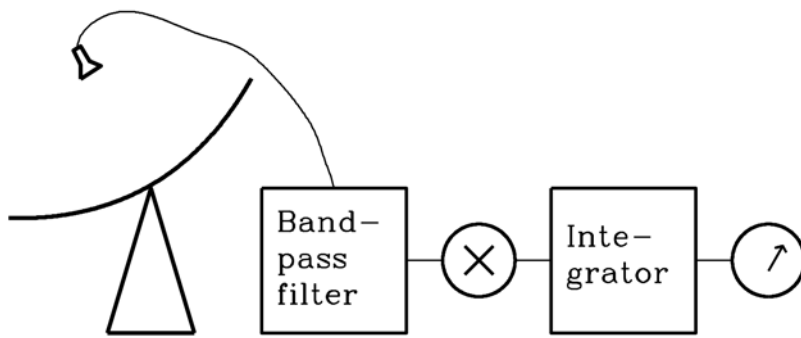
$$\nu_{\text{RF}} - \frac{\triangle \nu_{\text{RF}}}{2} \text{ to } \nu_{\text{RF}} + \frac{\triangle \nu_{\text{RF}}}{2},$$

where $\triangle \nu_{\text{RF}}$ is the receiver **bandwidth**. For example, the receivers used on the 300-foot telescope to make the $\lambda \approx 6$ cm continuum survey of the northern sky had a center radio frequency $\nu_{\text{RF}} \approx 4.85 \times 10^9$ Hz a bandwidth $\triangle \nu_{\text{RF}} \approx 6 \times 10^8$ Hz.

The simplest radiometer consists of four stages in series:

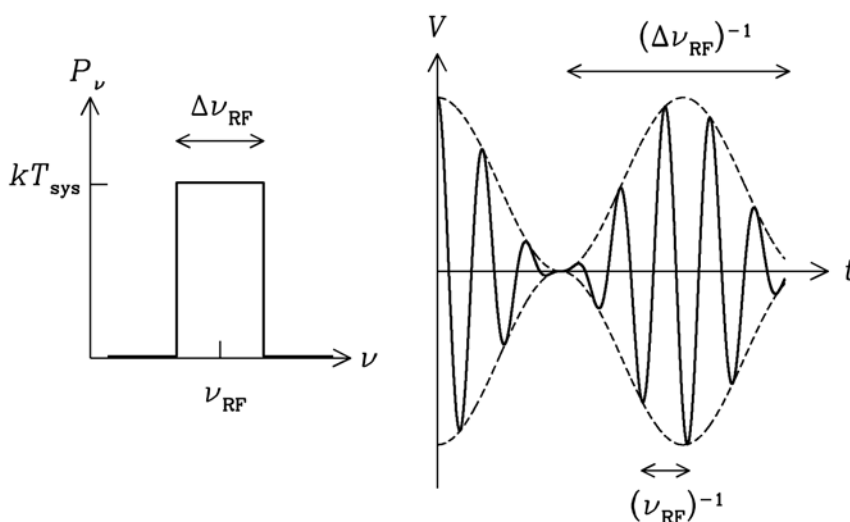
- (1) an ideal (lossless) **bandpass filter** that passes input noise only in the desired frequency range,
- (2) an ideal **square-law detector** whose output voltage is proportional to the square of its input voltage; that is, its output voltage is proportional to its input power,
- (3) a signal averager or **integrator** that smoothes out the rapidly fluctuating detector output, and

(4) a voltmeter or other device to measure and record the smoothed voltage.



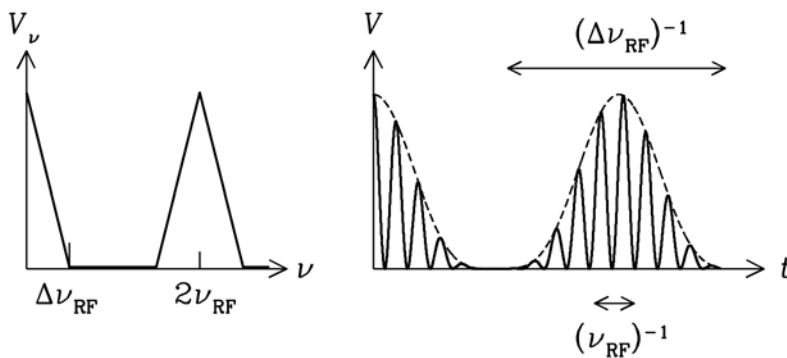
The simplest radiometer filters the broadband noise coming from the telescope, multiplies the filtered voltage by itself (square-law detection), smooths the detected voltage, and measures the smoothed voltage. The function of the detector is to convert the noise voltage, which has zero mean, to noise power, which is proportional to the square of voltage.

After passing through an input filter of width $\Delta\nu_{\text{RF}} \ll \nu_{\text{RF}}$ the noise voltage is no longer completely random; it looks more like a sine wave of frequency $\approx \nu_{\text{RF}}$ whose amplitude envelope varies randomly on time scales $\Delta t \approx (\Delta\nu_{\text{RF}})^{-1} \gg \nu_{\text{RF}}^{-1}$. The positive and negative envelopes are similar so long as $\Delta\nu_{\text{RF}} \ll \nu_{\text{RF}}$.



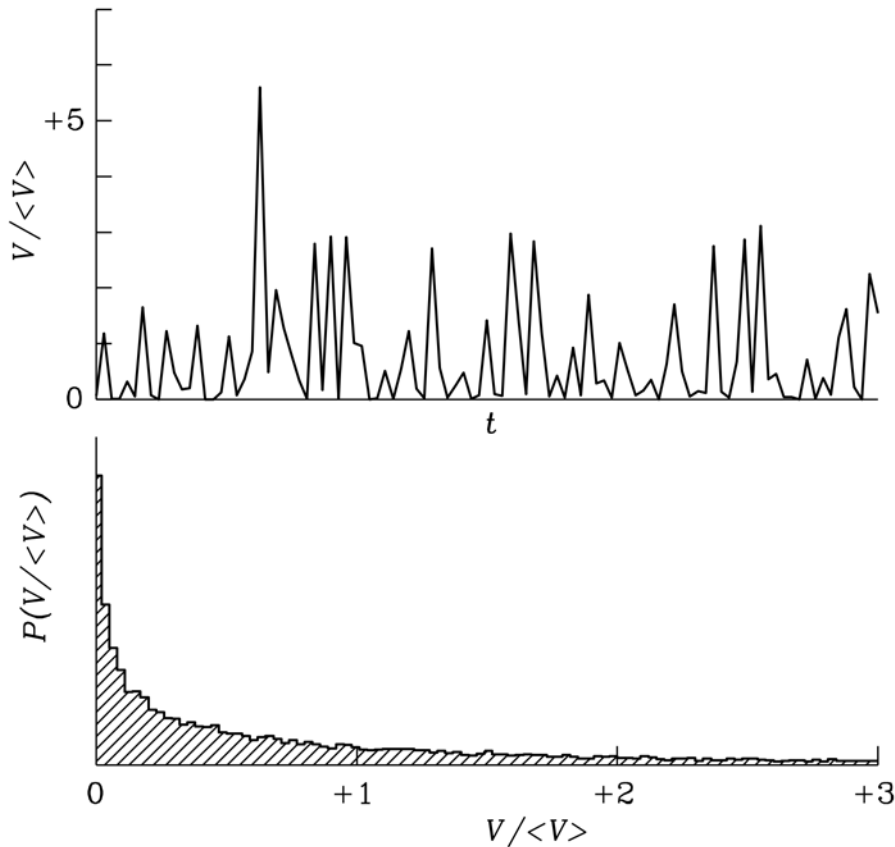
The voltage output of the filter with center frequency ν_{RF} and bandwidth $\Delta\nu_{\text{RF}} < \nu_{\text{RF}}$ is a sinusoid with frequency ν_{RF} whose envelope (dashed curves) fluctuates on time scales $(\Delta\nu_{\text{RF}})^{-1} > (\nu_{\text{RF}})^{-1}$.

The filtered output is sent to a square-law detector, a device whose output voltage is proportional to the square of its input voltage, so the detector output voltage is proportional to its input power. For a narrowband (quasi-sinudoidal) input voltage $V_i \approx \cos(2\pi\nu_{\text{RF}}t)$ at frequency ν_{RF} , the detector output voltage would be $V_o \propto \cos^2(2\pi\nu_{\text{RF}}t)$. This can be rewritten as $[1 + \cos(4\pi\nu_{\text{RF}}t)]/2$, a function whose mean value equals the average power of the input signal. In addition to the DC (zero-frequency component) there is an oscillating component at twice ν_{RF} . The detector output spectrum for a finite bandwidth $\Delta\nu_{\text{RF}}$ and a typical waveform are shown below:



The output voltage of a square-law detector is proportional to the square of the input voltage. It is always positive, so its mean (DC component) is positive and is proportional to the input power. The high frequency ($\nu \approx 2\nu_{\text{RF}}$) fluctuations contain no useful information about the source and are filtered out by the next stage.

The oscillations under the envelope approach zero every $\Delta t \approx (2\nu_{\text{RF}})^{-1}$. Thus the oscillating component of the detector output is centered near the frequency $2\nu_{\text{RF}}$. The detector output also has frequency components near zero (DC) since the mean output voltage is greater than zero.



The output voltage histogram of a square-law detector fed with Gaussian noise is peaked sharply near zero and has a long positive tail. The mean detected voltage $\langle V \rangle$ equals the mean squared input voltage, and the rms of the detected voltage is $2^{1/2}\langle V \rangle$. For a detailed derivation of the detector output distribution and its rms, click [here](#).

Both the rapidly varying component at frequencies near $2\nu_{\text{RF}}$ and its envelope vary on time scales that are normally much shorter than the time scales on which the average signal power ΔT varies. The unwanted rapid variations can be suppressed by taking the arithmetic mean of the detected envelope over some time scale $\tau \gg (\Delta\nu_{\text{RF}})^{-1}$ by integrating or averaging the detector output. This integration might be done electronically by smoothing with an RC (resistance plus capacitance) filter or numerically by sampling and digitizing the detector output voltage and then computing its running mean.

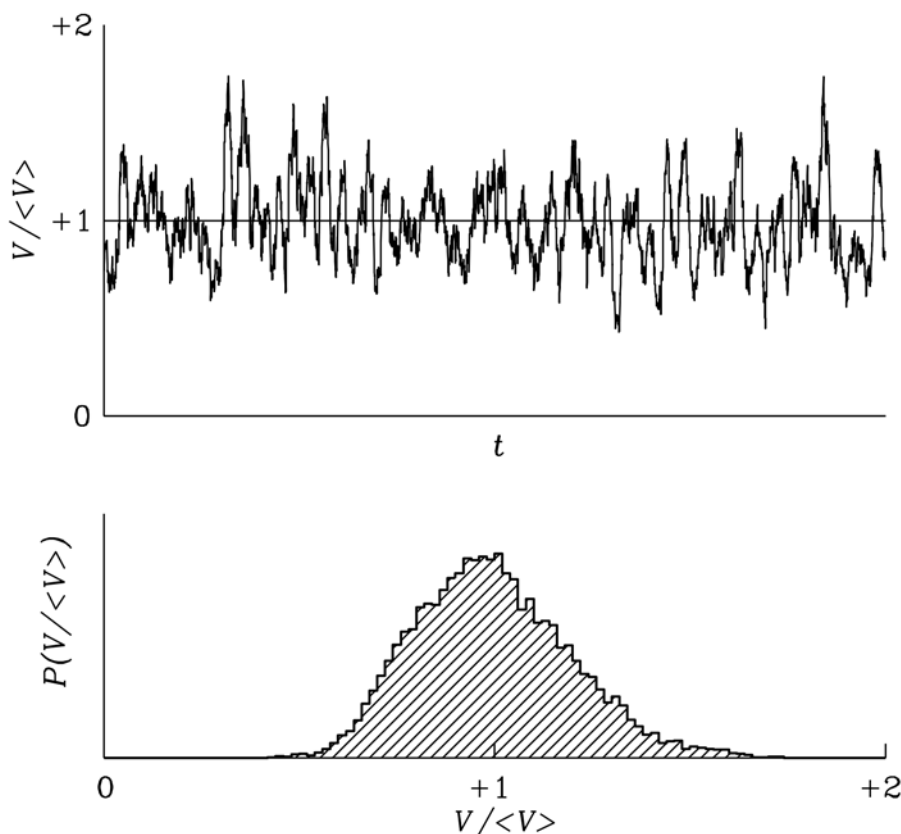
Integration greatly reduces the receiver output fluctuations. In the time interval τ there are $N = 2\Delta\nu_{\text{RF}}\tau$ independent samples of the total noise power T_{sys} , each of which has an rms error $\sigma_T \approx 2^{1/2}T_{\text{sys}}$. The rms error in the average of $N \gg 1$ independent samples is reduced by the factor \sqrt{N} , so the rms receiver output fluctuation σ_T is only

$$\sigma_T = \frac{2^{1/2} T_{\text{sys}}}{N^{1/2}} .$$

In terms of bandwidth $\Delta\nu_{\text{RF}}$ and integration time τ ,

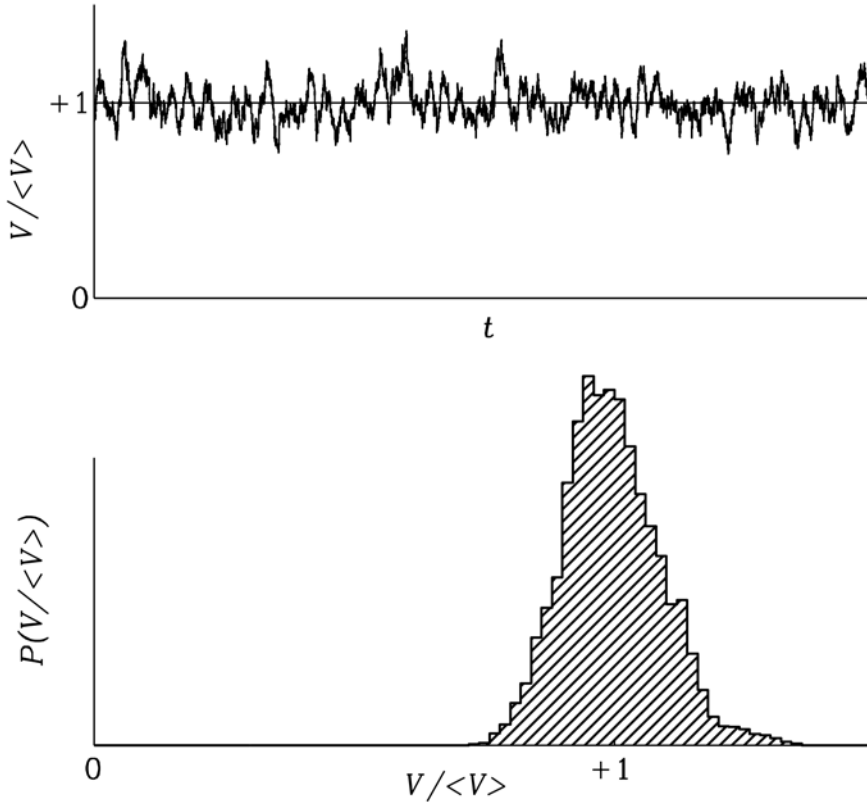
$$\sigma_T \approx \frac{T_{\text{sys}}}{\sqrt{\Delta\nu_{\text{RF}} \tau}} \quad (3E3)$$

after smoothing. The central limit theorem of statistics implies that heavily smoothed ($\Delta\nu_{\text{RF}} \tau \gg 1$) output voltages also have a nearly Gaussian amplitude distribution. This important equation is called the **ideal radiometer equation** for a total-power receiver. The weakest detectable signals ΔT only have to be several (typically five) times the output rms σ_T given by the radiometer equation, not several times the total system noise T_{sys} . The product $\Delta\nu_{\text{RF}} \tau$ may be quite large in practice (10^8 is not unusual), so signals as faint as $\Delta T \sim 5 \times 10^{-4} T_{\text{sys}}$ would be detectable. The two figures below illustrate the effects of smoothing the detector output by taking running means of lengths $N = 50$ and $N = 200$ samples.



The smoothed output voltage from the integrator varies on time scale τ

with small amplitude σ_T given by the radiometer equation. The top part of this figure shows the detected voltage smoothed by an $N = 50$ sample running mean, and the bottom part shows the amplitude distribution of the smoothed voltage. This amplitude distribution has mean $\langle V \rangle$ and rms $(2/N)^{1/2} \langle V \rangle = 0.2 \langle V \rangle$. As N grows, the smoothed amplitude distribution approaches a Gaussian. The sampling theorem states that $N = 2 \Delta \nu_{\text{RF}} \tau$ so $\Delta \nu_{\text{RF}} \tau = 25$ for this example.



When the same detector output is smoothed over $N = 200$ samples instead of $N = 50$ samples, the mean remains the same but the rms falls by a factor of $4^{1/2} = 2$ to $0.1 \langle V \rangle$. In this example $\Delta \nu_{\text{RF}} \tau = 100$.

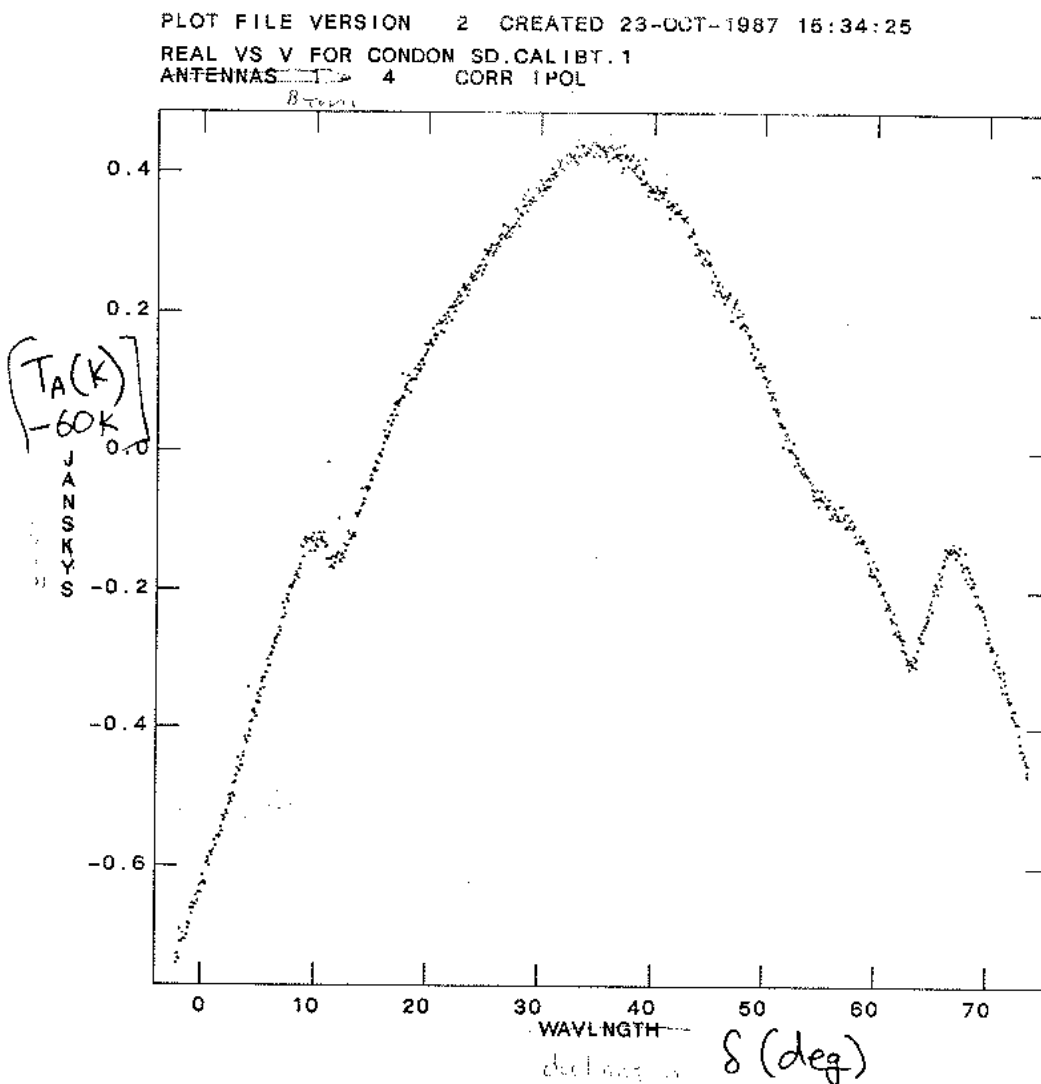
Example: The $\nu \approx 4.85$ GHz ($\lambda \approx 6$ cm) northern sky survey made with the 300-foot (91 m) telescope.

This survey used total-power radiometers very similar to the radiometer described above, but with multistage RF amplifiers that simultaneously amplified and filtered the input signals. The telescope was driven up and down in elevation at its slew rate $\pm 10^\circ$ per minute = 10 arcmin per second of time. The beamwidth was

$$\theta_{\text{HPBW}} \approx \frac{1.2\lambda}{D} = \frac{1.2c}{\nu_{\text{RF}} D}$$

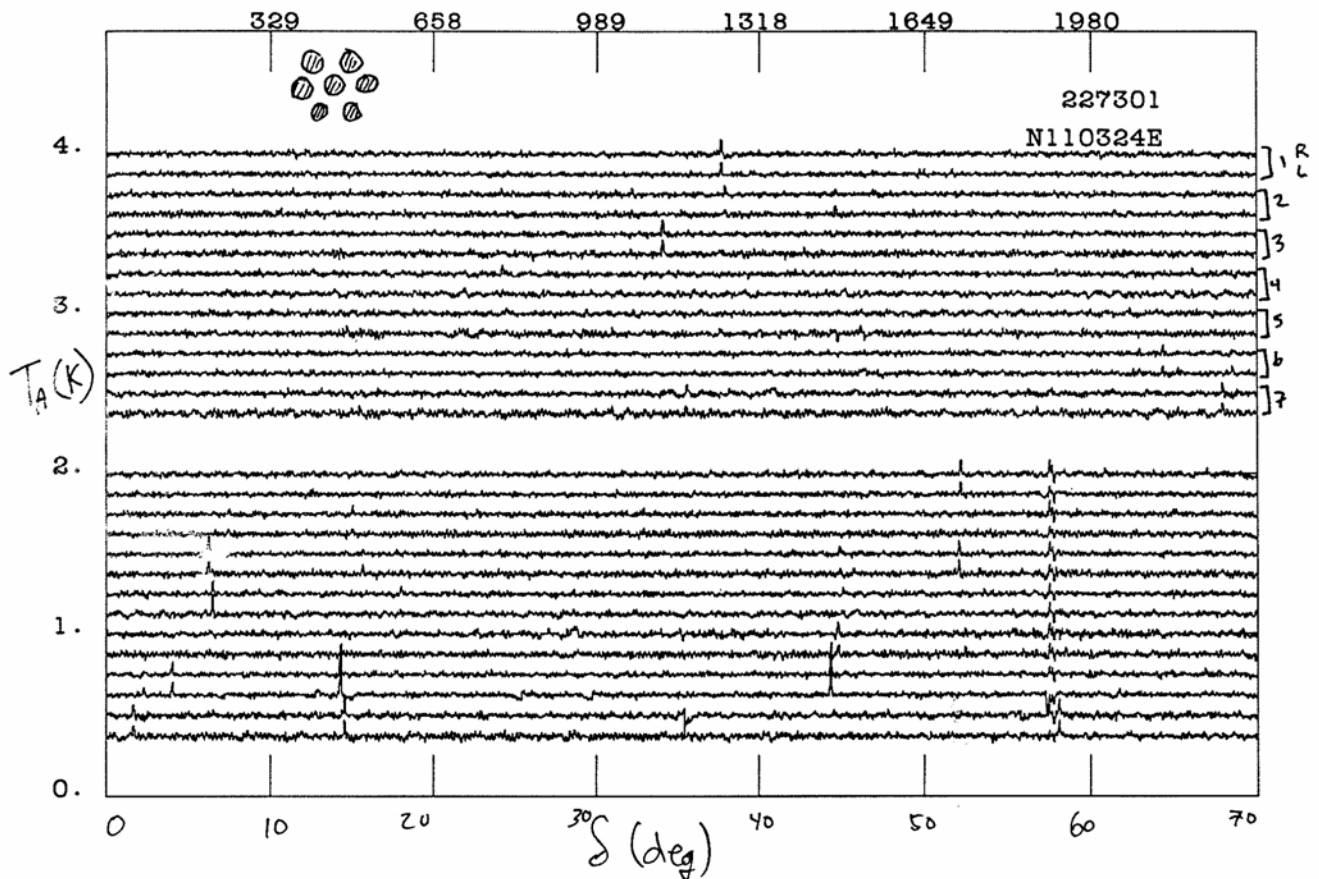
$$\theta_{\text{HPBW}} \approx \frac{1.2 \times 3 \times 10^8 \text{ m s}^{-1}}{4.85 \times 10^9 \text{ Hz} \times 91 \text{ m}} \approx 8.2 \times 10^{-4} \text{ rad} \approx 2.8 \text{ arcmin}$$

The scanning time between half-power points was thus ≈ 0.3 s. The data were integrated and sampled every $\tau = 0.1$ s, so there were ≈ 3 samples per half-power beamwidth. A subset of the samples taken from one receiver during one scan covering the declination range $\delta \approx -2^\circ$ to $\delta \approx +73^\circ$ is shown.



The intensity scale has been calibrated in Kelvins, and the large mean $T_{\text{sys}} \approx 60$ K has been subtracted. By far the biggest time-dependent signal (spanning a range of about 1 K) is caused by ground radiation entering the prime-focus feed via leakage through the reflector mesh and spillover. Fortunately, this unwanted ground signal varies smoothly with telescope elevation, so subtracting a short (about 40 arcmin long) running-median

baseline takes out the spillover signal without removing compact radio sources. The outputs from all 14 receiver channels (7 beams \times 2 polarizations/beam) after baseline subtraction are shown in the next viewgraph. Only now are the faint radio sources visible above the noise fluctuations.



Data from all 14 receivers after subtraction of running-median baselines. Sources appear as spikes in both polarization channels (R and L) of one or two beams. Interference is usually visible in all 14 receivers simultaneously.

The rms noise observed is consistent with the prediction of the total-power radiometer equation:

$$\sigma_T \approx \frac{T_{\text{sys}}}{\sqrt{\Delta\nu_{\text{RF}} T}} \approx \frac{60 \text{ K}}{\sqrt{6 \times 10^8 \text{ Hz} \times 0.1 \text{ s}}} \approx 0.008 \text{ K}$$

Some caveats

The ideal radiometer equation suggests that the sensitivity of a radio observation improves as $\tau^{1/2}$ forever. In practice, systematic errors set a floor to the noise level that can be reached. Receiver gain changes, erratic fluctuations in atmospheric emission, or "confusion" by the unresolved background of continuum radio sources usually limit the sensitivity of single-dish continuum observations.

Gain instability

Note that the output voltage of a total-power receiver is directly proportional to the overall gain G of the receiver:

$$P_\nu = GkT_{\text{sys}}$$

If G isn't perfectly constant, the change in output

$$\Delta P_\nu = \Delta GkT_{\text{sys}}$$

caused by a **gain fluctuation** ΔG produces a false signal

$$\Delta T_G = T_{\text{sys}} \left(\frac{\Delta G}{G} \right)$$

that is indistinguishable from a comparable change ΔT in the system noise temperature produced by an astronomical source. Since receiver gain fluctuations and noise fluctuations are independent random processes, their **variances** (the variance is the square of the rms) add, and the total receiver output fluctuation becomes:

$$\sigma_{\text{total}}^2 = \sigma_{\text{noise}}^2 + \sigma_G^2$$

$$\sigma_{\text{total}}^2 = T_{\text{sys}}^2 \left[\frac{1}{\Delta\nu_{\text{RF}}\tau} + \left(\frac{\Delta G}{G} \right)^2 \right]$$

The **practical total-power radiometer equation** is thus:

$$\sigma_T \approx T_{\text{sys}} \left[\frac{1}{\Delta\nu_{\text{RF}}\tau} + \left(\frac{\Delta G}{G} \right)^2 \right]^{1/2} \quad (3E4)$$

Clearly, gain fluctuations will significantly degrade the sensitivity unless

$$\left(\frac{\Delta G}{G}\right) \ll \frac{1}{\sqrt{\Delta\nu_{\text{RF}} \tau}}$$

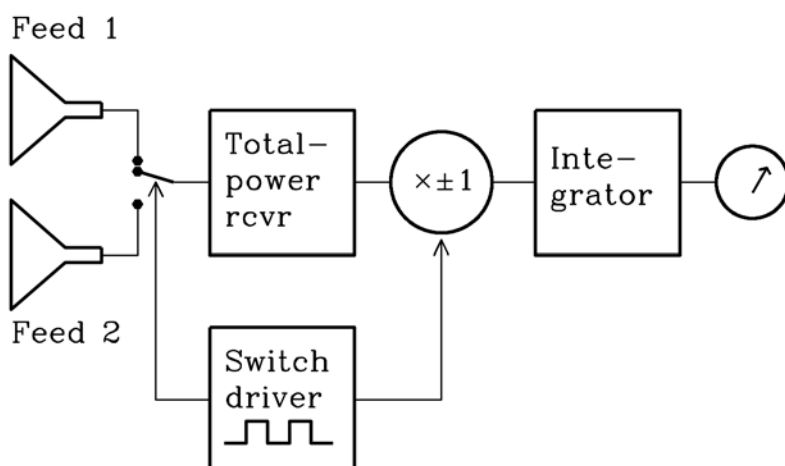
For example, the 5 GHz receiver used to make the sky survey with the 300-foot telescope had $\Delta\nu_{\text{RF}} \approx 6 \times 10^8 \text{ Hz}$ and $\tau \approx 0.1 \text{ s}$, so the fractional gain fluctuations on time scales up to a few seconds (the time to scan one baseline length) had to satisfy

$$\frac{\Delta G}{G} \ll \frac{1}{\sqrt{6 \times 10^8 \text{ Hz} \times 0.1 \text{ s}}} = 1.3 \times 10^{-4}$$

This is difficult to achieve in practice. Gain fluctuations typically have a " $1/f$ " power spectrum, where f is the postdetection frequency, so they are larger on longer time scales and increasing τ eventually results in a higher noise level. The gain stability of a receiver is often specified by the " $1/f$ knee" f_{knee} , the postdetection frequency at which $\sigma_{\text{noise}} = \sigma_G$. Integrations longer than $\tau \approx 1/(2\pi f_{\text{knee}})$ will likely increase the noise level.

Fluctuating atmospheric emission

Fluctuations in atmospheric emission also add to the noise in the output of a simple total-power receiver. Water vapor is the main culprit because it is not well mixed in the atmosphere, and noise from water-vapor fluctuations can be a significant problem at frequencies of $\sim 5 \text{ GHz}$ and up. One way to minimize the effects of fluctuations in both receiver gain and atmospheric emission is to make a *differential* measurement by comparing signals from two adjacent feeds. The method of switching rapidly between beams or loads is called **Dicke switching** after Robert Dicke, its inventor.



Block diagram of a beamswitching differential radiometer. The total-power

receiver is switched between two feeds, one pointing at the source and one displaced by a few beamwidths to avoid the source but measure emission from nearly the same sample of atmosphere. The output of the total-power receiver is multiplied by +1 when the receiver is connected to the on-source feed and by −1 when it is connected to the reference feed. Fluctuations in atmospheric emission and in receiver gain are effectively suppressed for frequencies below the switching rate, which is typically in the range 10 to 1000 Hz.

If the system temperatures are T_1 and T_2 in the two positions of the switch, then the receiver output is proportional to $T_1 - T_2 \ll T_1$ and the effect of gain fluctuations is only

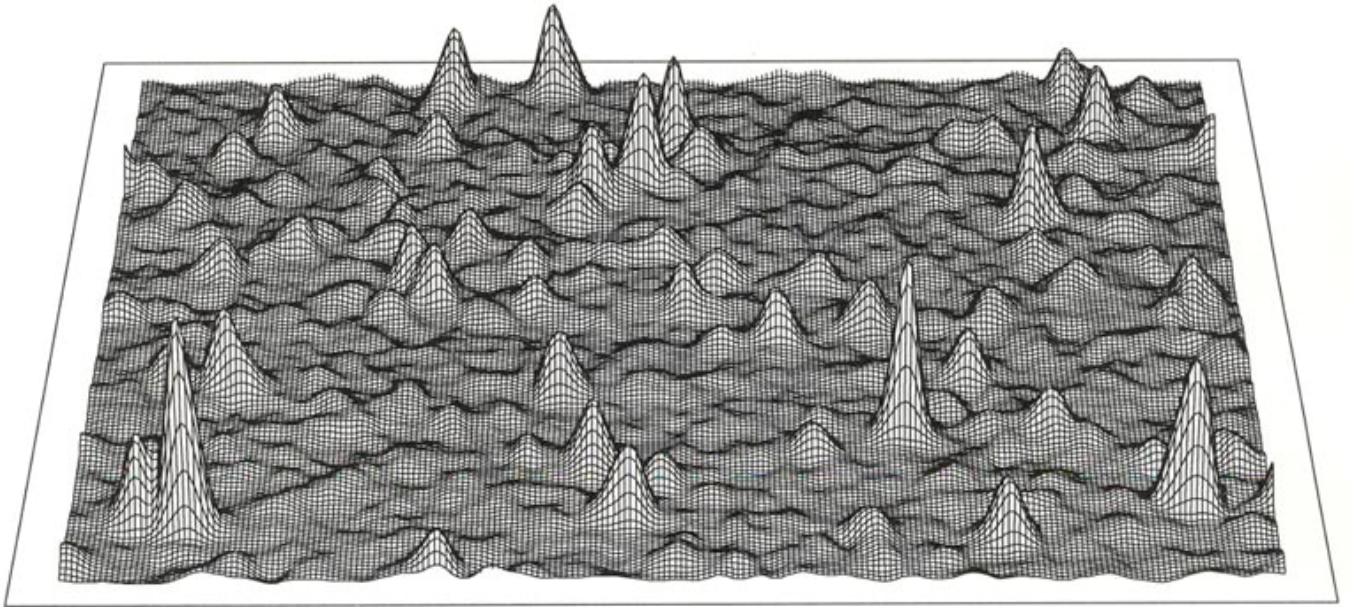
$$\Delta T_G \approx (T_1 - T_2) \frac{\Delta G}{G} \ll T_1 \frac{\Delta G}{G} .$$

Likewise, the atmospheric emission in two nearly overlapping beams through the troposphere is nearly the same, so most of the tropospheric fluctuations cancel out. The main drawback with Dicke switching is that the receiver output fluctuations, relative to the source signal in a single beam, are doubled, so the radiometer equation for a Dicke switching receiver is:

$$\sigma_T = \frac{2T_{\text{sys}}}{\sqrt{\Delta\nu_{\text{RF}} \tau}} \quad (3E5)$$

Confusion

Single-dish radio telescopes have large collecting areas but relatively poor angular resolution at long wavelengths. Nearly all discrete continuum sources are extragalactic and extremely distant, so they are distributed randomly and isotropically on the sky. The sky-brightness fluctuations caused by numerous faint sources in the telescope beam are called **confusion**, and confusion usually limits the sensitivity of single-dish continuum observations at frequencies below $\nu \sim 10$ GHz.

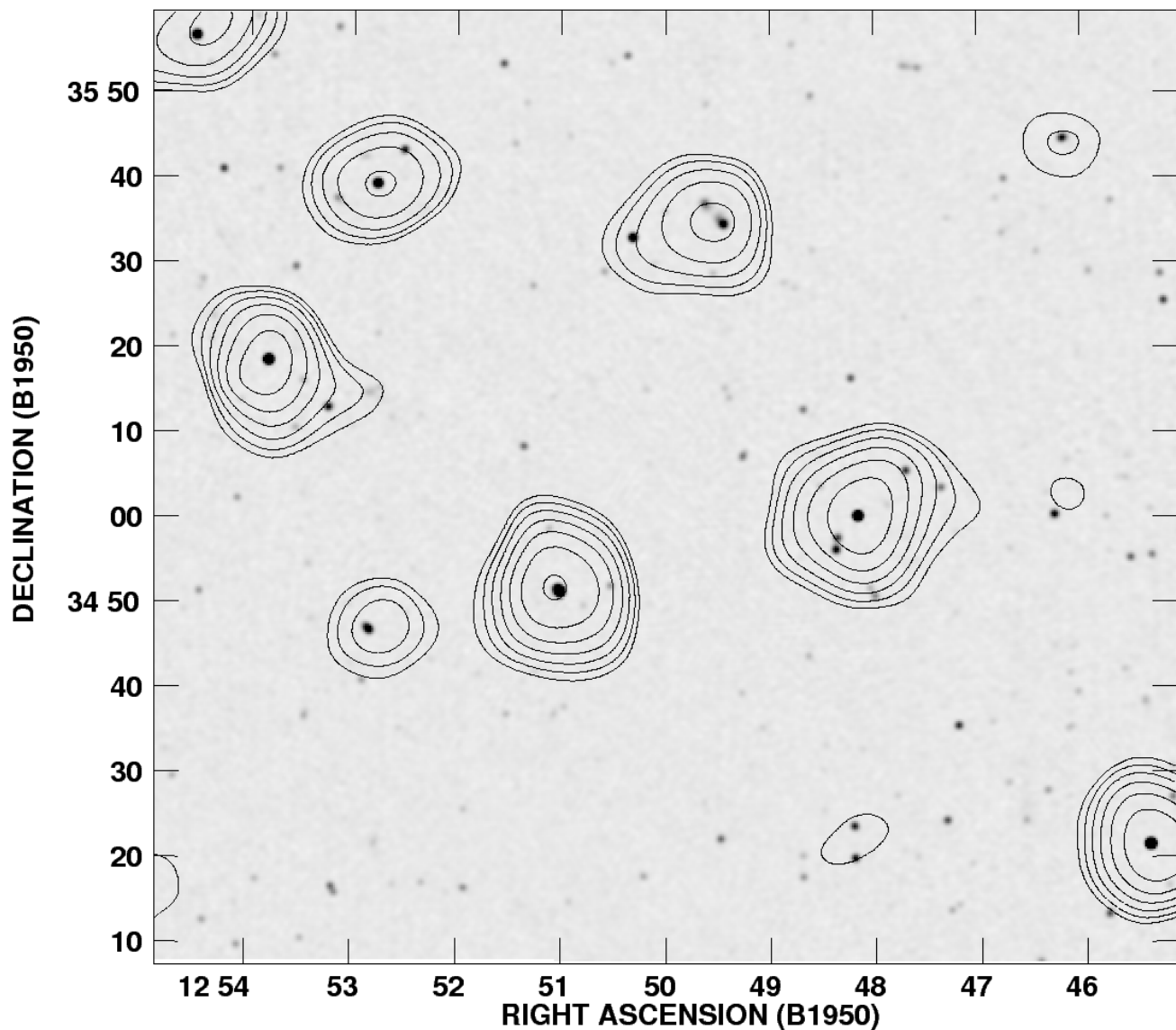


This profile plot covers 45 deg^2 of sky near the north Galactic pole, as imaged with $\theta = 12 \text{ arcmin}$ resolution at $\nu = 1.4 \text{ GHz}$ with the former 300-foot radio telescope in Green Bank. The strongest source shown has a flux density $S \approx 1.5 \text{ Jy}$, and the low-level brightness fluctuations with rms $\sigma \approx 0.02 \text{ Jy beam}^{-1}$ are caused by the superposition of numerous faint sources, not receiver noise. Consequently, individual sources fainter than $S \approx 0.1 \text{ Jy}$ cannot be detected reliably in these data.

The amplitude distribution of confusion is distinctly non-Gaussian, with a long positive-going tail. Nonetheless, the rms confusion σ_c is a widely used parameter for specifying the width of the confusion distribution. At cm wavelengths, the rms confusion in a telescope beam with FWHM θ is observed to be

$$\left(\frac{\sigma_c}{\text{mJy beam}^{-1}} \right) \approx 0.2 \left(\frac{\nu}{\text{GHz}} \right)^{-0.7} \left(\frac{\theta}{\text{arcmin}} \right)^2 \quad (3E6)$$

Individual sources fainter than about $5\sigma_c$ cannot be detected reliably. Most continuum observations of faint sources at frequencies below $\nu \sim 10 \text{ GHz}$ are made with interferometers instead of single dishes because interferometers can synthesize much smaller beamwidths θ and hence have significantly lower confusion limits.



This contour plot shows a 4 deg^2 sub-region from the area covered by the profile plot above, as imaged with $\theta = 12 \text{ arcmin}$ resolution at $\nu = 1.4 \text{ GHz}$ with the former 300-foot radio telescope in Green Bank. The lowest contour level is $45 \text{ mJy beam}^{-1} \approx 2\sigma_c$ and successive contours are spaced by factors of $2^{1/2}$ in brightness, so sources with fewer than four contours are below the confusion limit. The underlying gray-scale plot is a 1.4 GHz VLA image made with $\theta = 45 \text{ arcsec}$ resolution. Some of the faint sources seen by the 300-foot telescope are "real" and some are blends of two or more fainter sources resolved by the VLA.

Confusion by steady continuum sources has a much smaller effect on observations of spectral lines or rapidly varying sources such as pulsars.

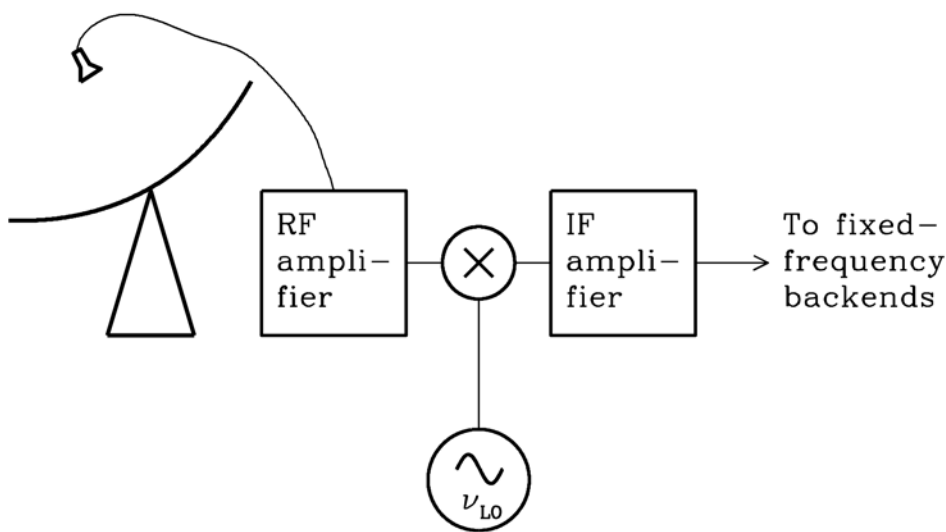
Superheterodyne Receivers

Few actual radiometers are as simple as those described above. Nearly all practical radiometers are **superheterodyne** receivers, in which the RF amplifier is followed by a **mixer** that multiplies the RF signal by a sine

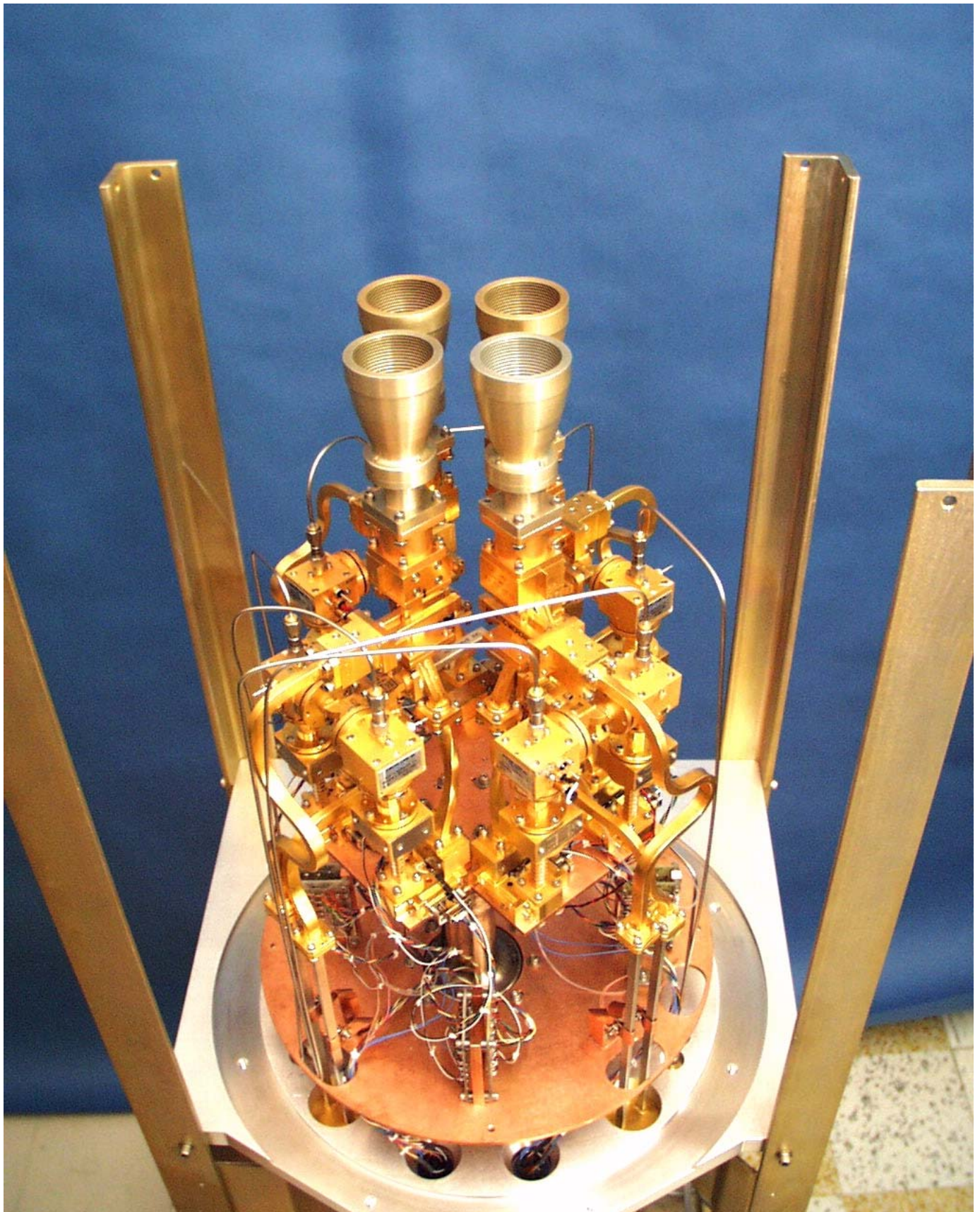
wave of frequency ν_{LO} generated by a **local oscillator** (LO). The product of two sine waves contains the sum and difference frequency components

$$2 \sin(2\pi\nu_{\text{LO}}t) \times \sin(2\pi\nu_{\text{RF}}t) = \cos[2\pi(\nu_{\text{LO}} - \nu_{\text{RF}})t] - \cos[2\pi(\nu_{\text{LO}} + \nu_{\text{RF}})t] .$$

The difference frequency is called the **intermediate frequency** (IF). The advantages of superheterodyne receivers include doing most of the amplification at lower frequencies ($\nu_{\text{IF}} \leq \nu_{\text{RF}}$), which is usually easier, and precise control of the ν_{RF} range covered via tuning *only* the local oscillator so that **back-end** devices following the untuned IF amplifier, multichannel filter banks or digital spectrometers for example, can operate over fixed frequency ranges.



Block diagram of a simple superheterodyne receiver. Only the local oscillator is tuned to change the observing frequency range.



The GBT Q-band (ν_{RF} from 40 to 52 GHz) receiver showing the 20 K cryogenic stage with four feed horns, noise calibration sources, RF amplifiers, LO, mixers, and cables leading to the ν_{IF} 4 to 8 GHz IF amplifiers. [Image credit](#)

